NUMERICAL INVESTIGATION OF FLOW OF GENERALIZED NEWTONIAN FLUIDS IN DOUBLE-SCALE POROSITY COMPOSITE REINFORCEMENTS

E. Syerko*[1], C. Binetruy[1], A. Leygue[1], S. Comas-Cardona[1], A. Trameçon[2]

[1]*Research Institute in Civil Engineering and Mechanics (GeM), UMR CNRS 6183, École Centrale de Nantes, 1 rue de la Noë, BP 92101, 44321 Nantes Cedex 3, France*

[2]*ESI Group, Parc d'Affaires SILIC, 99 rue des Solets, BP 80112, 94513 Rungis Cedex, France*

* *Corresponding Author: olena.syerko@ec-nantes.fr*

Keywords: Liquid Composite Molding, textile reinforcement, Brinkman equation, Proper Generalized Decomposition, Generalized Newtonian fluids,

Abstract

In order to model the resin flow through the complex double-scale porosity architecture of textile reinforcements, requiring rich numerical discretization, the Proper Generalized Decomposition (PGD) technique applied to the Stokes and Brinkman equations is employed in this study. The performed parametric study allows to identify the ratios of parameters for which the Newtonian flow within the fiber bundles at micro-scale can be neglected compared to the flow between the fiber bundles (yarns) at meso-scale. Owing to the concept of the PGD, the parametric study was realized in one-shot calculation for a range of inter-yarn distances related to the permeability values without increasing much the computational cost. Besides, modeling of the generalized Newtonian flow using the Stokes equation was performed, and distinguished the cases when the fluid shows up the shear-thinning behavior only in the voids between the yarns, and not inside the yarns, where thus can be neglected.

1. Introduction

These days new reactive and non-reactive thermoplastic resins designed for the high speed manufacturing in the automotive industry arrive at the market of polymer textile composites. The advantage of these thermoplastic polymers is their low viscosity, which allows to reduce the preform filling time during the liquid composite molding. At the same time, their viscosity dependence on the shear strain rate makes their behavior to gain a non-Newtonian character (also called generalized Newtonian behavior). Particularly, the flow of pseudoplastic fluids – the mostly widespread class of generalized Newtonian fluids – through the textile reinforcements will be considered in the sequel.

The fibrous reinforcements of composite materials own a complex multi-scaled porous structure. This makes the resin during the liquid composite molding processes flow not only in the voids between the meso-scale constituents of reinforcements – tows, but also penetrate the tows (fiber bundles), and flow in the channels between the micro-scale constituents – fibers, composing the tows. However, nowadays the resin flow, even with the Newtonian behavior, through

textile preforms, characterized by the double-scale porosity, is most often addressed with the help of models accounting only for the macro-scale behavior, e.g. the well-known Darcy's law, which allows to obtain only the generalized volume averaged flow velocity. Therefore, in this study, before complexifying the flow by the non-Newtonian behavior, the Brinkman equation is employed for the Newtonian flow in order to, firstly, address correctly two types of porosities – voids at the microscopic and mesoscopic scales. Secondly, to ensure the continuity of the velocity and stress fields at the boundary between domains yarn-resin (Fig. 1). Thirdly, to account for the viscous shear in the fluid domain as well (as opposed to the Darcy's law). Since the complex double-scale architecture of textile reinforcements may cause the resin flow field to acquire a fully 3D character, the Brinkman equation is suggested to be solved here by the Proper Generalized Decomposition (PGD) numerical technique [1]. Based on the principle of separation of variables from each other, it allows to use very fine meshes without increasing exponentially the computational time, which is the case for the classical numerical methods when the problem dimensionality is increased. Moreover, with the help of the PGD the parametric study of the influence of a range of parameters on the resultant local velocity field will be realized performing only one calculation.

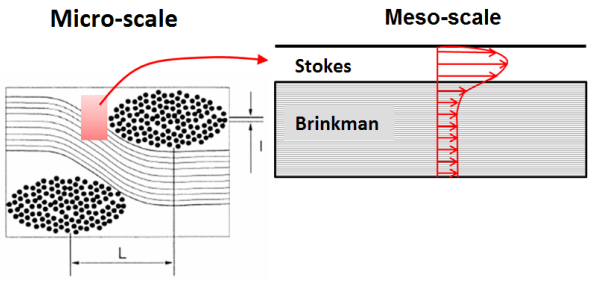

Figure 1. Modeling of the flow in double-scale porosity fibrous reinforcement viewed as a porous medium

Next step of this study is to pass on from the Newtonian behavior of resin flowing through the fibrous preform to modeling the non-Newtonian resin flow. The three-dimensional Stokes non-Newtonian flow through the fiber bundles will be solved by the PGD technique using the Carreau-Yasuda model for addressing the viscosity dependence on the shear rate. The influence of different geometrical and physical parameters on the resultant flow field and the viscosity distribution will be analyzed.

2. Resolution methodology

In order to overcome the limitations of the macroscopic prediction (e.g. by the Darcy's law) of the resin flow through the textile reinforcements, giving as a result the generalized volume averaged flow velocity, the Brinkman equation [2], which takes into account the local inter-yarn, as well as the intra-yarn flow, is employed in this study:

$$\phi \nabla p = \mu \nabla^2 \upsilon_{\mathbf{A}} - \phi \mu K^{-1} \cdot \upsilon_{\mathbf{A}}, \tag{1}$$

where $\upsilon_{\mathbf{A}}$ is the fluid volume averaged velocity, which is equal to the product of the intrinsic average fluid velocity $\mathbf{u}$ and the porosity ϕ: $\upsilon_{\mathbf{A}} = \phi \mathbf{u}$; μ is the fluid viscosity; p is the pressure; K is the permeability of the porous domain. Thus the flow between the fiber bundles is described by the first (Stokes) term of the Brinkman equation, while the flow through the micro-channels

of the fiber bundle is mostly addressed by the second (Darcy) term. The system of momentum and mass conservation equations was solved by the PGD technique with the help of the pseudo-compressibility method to link the velocity and pressure fields. The corresponding weak form of the problem reads:

$$\int_\Omega \nabla \cdot \mathbf{u}^* \cdot \phi \nabla \cdot \mathbf{u} + \lambda\mu \,\mathrm{grad}\,\mathbf{u}^* : \mathrm{grad}\,\mathbf{u} d\Omega + \int_\Omega \mathbf{u}^* \cdot \phi\lambda K^{-1}\mu \cdot \mathbf{u} d\Omega = 0, \tag{2}$$

for all test functions $\mathbf{u}^*$ selected in an appropriate functional space; here λ is the penalization factor of the pseudocompressibility method: $\lambda << 1$. According to the PGD principles, the intrinsic fluid velocity field $\mathbf{u}(x, y, z)$ in three-dimensional space is sought in the form of the separated representation:

$$\mathbf{u}(x,y,z) = \begin{pmatrix} u(x,y,z) \\ v(x,y,z) \\ \omega(x,y,z) \end{pmatrix} \approx \sum_{j=1}^{N} \begin{pmatrix} u_j(x) \cdot u_j(y) \cdot u_j(z) \\ v_j(x) \cdot v_j(y) \cdot v_j(z) \\ \omega_j(x) \cdot \omega_j(y) \cdot \omega_j(z) \end{pmatrix}, \tag{3}$$

where N is the number of modes – functional products in the sum – sufficient to satisfy the convergence criterion for the accurate representation of the solution. Each term of the expansion is computed in the iterative procedure by applying an alternating direction fixed point algorithm. Thus the original 3D problem defined over $\Omega = \Omega_x \times \Omega_y \times \Omega_z$ is transformed within the PGD framework into a series of decoupled one-dimensional problems formulated in Ω_x, Ω_y, and Ω_z. The PGD resolution procedure is explained in details in the work [1].

The correctness of the contribution of the Stokes term in the Brinkman equation was validated with a Poiseuille flow in a channel against its exact solution, as well as on the widespread numerical test-case of the lid driven cavity.

In order to predict the flow through an array of aligned fiber bundles with elliptical (or more generally arbitrary) cross-sections (Fig. 2a), a more complex separated representation in the form of product of 2D and 1D functions dependent on the spatial coordinates is needed, e.g. for the first velocity component the representation will be $\sum_{j=1}^{N} u_j(x, y) \cdot u_j(z)$. The separated form (3) allows to address only simple Cartesian geometries.

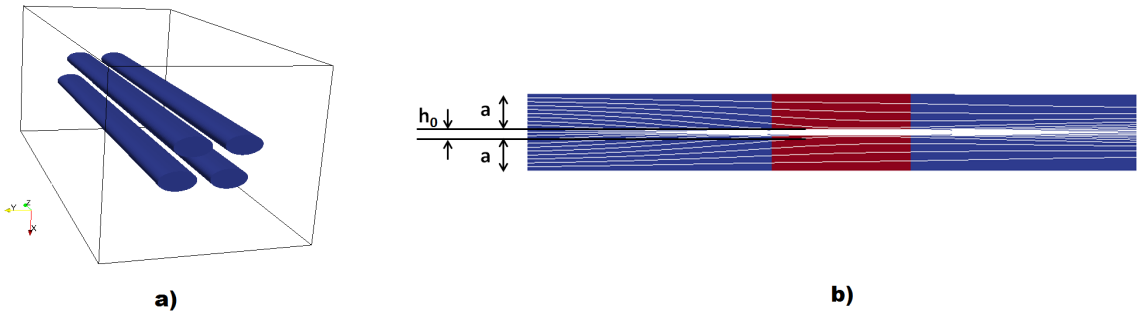

Figure 2. a) Three-dimensional domain of fiber bundles realized via 2D x 1D separation; b) sketch of the investigated flow domain with the varying inter-yarn distance h_0.

3. Parametrized solution of Brinkman equation

It is of interest to know if in the flow modeled by the Brinkman equation, taking into account both micro- and meso-effects, the contributions from both scales mechanisms are equivalent, or if there are some cases where the contribution from the flow rate within the micro-structure is negligible. Using the potential of the Proper Generalized Decomposition we can solve the problem at once for a range of parameters [3], selecting the parameter of interest here to be the inter-yarn distance h. It defines the width of the meso-channel for the flow perpendicular to the axes of aligned yarns, which is considered here (Fig. 2b). The solution of the Brinkman equation after the penalization is now sought in the form:

$$\mathbf{u}(x, y, s, h) \approx \sum_{j=1}^{N} \mathbf{u}_j(x) \cdot \mathbf{u}_j(y) \cdot \mathbf{u}_j(s) \cdot \mathbf{u}_j(h), \tag{4}$$

where s is the third space coordinate: $s \rightarrow z$, z being the function of s and h as follows.

$$z = \begin{cases} s & s \in [0, a] \\ (s-a) \cdot h/h_0 + a & s \in (a, a+h_0) \\ s - h_0 + h & s \in [a+h_0, 2a+h_0] \end{cases} \tag{5}$$

where h_0 is a lower bound of the range of the investigated h – the minimal width of the channel; a is a size of the fibrous micro-structure in s-direction. s and h are independent coordinates in the chosen separated representation. Jacobian matrix owns the components 1 or $\frac{h}{h_0}$. The transformed weak form (2) will read:

$$\int_0^{x_{max}} \int_0^{y_{max}} \int_0^{s_{max}} \int_{h_{min}}^{h_{max}} (\nabla \cdot \mathbf{u}^* \cdot \phi \nabla \cdot \mathbf{u} + \lambda\mu \nabla \mathbf{u}^* : \nabla \mathbf{u} + \mathbf{u}^* \cdot \phi \lambda K^{-1} \mu \cdot \mathbf{u}) dx dy \frac{\partial z}{\partial s} ds dh = 0 \tag{6}$$

where the divergence and gradient of $\mathbf{u}$ contain the information from z-function. Consequently, the four-dimensional problem, with the parameter h as an extra-coordinate, is now decoupled into 1D x 1D x 1D x 1D problems and can be solved with the computational complexity of 1D problem. The classical numerical computation implies the resolution of a 3D problem for each particular value of the parameter. With the "on-line" particularization of the obtained "off-line" solution related to different ratios between the width of meso-voids between yarns and the permeability of the fibrous micro-structure of yarns the different phenomena and flow fields can be observed in post-processing.

The performed calculations confirmed that the flow rate enhancement **within** the fiber bundles cannot be neglected when either the permeability of fiber bundles K (at micro-scale) is relatively large, or the characteristic distance between the fiber bundles h (at meso-scale) is relatively small. The flow field strongly depends on the ratio between these two parameters, often referred to as Darcy number. It was found that when $K/h^2 < 10^{-3}$ – see (Fig. 3) – the flow inside the fiber bundles can be neglected with respect to the flow outside the fiber bundles, and the macroscopic volume averaged predictions of the flow field may be acceptable. However this condition is not always fulfilled in highly compacted fibrous reinforcements.

4. Generalized Newtonian flow through fibrous reinforcements

Since the viscosity in the second (Darcy) term of the Brinkman equation is not a physically defined quantity, but the value ensuring the continuity of velocity at the fluid/medium interface,

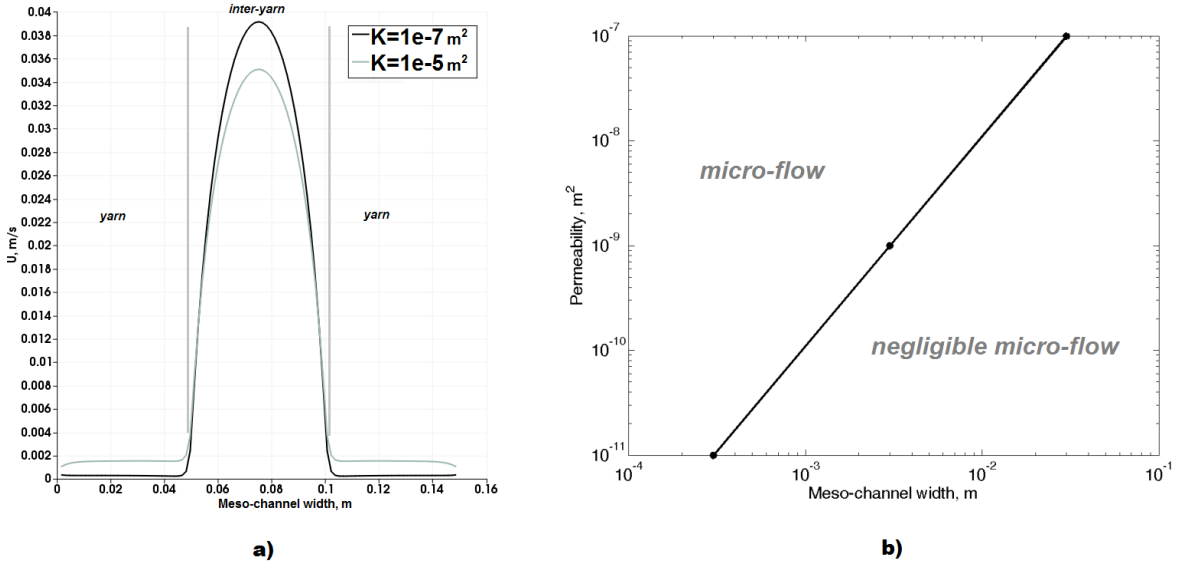

Figure 3. a) Velocity profiles with respect to different values of local (yarn) permeability; b) micro-permeability values versus the meso-channel width values.

the fibrous microstructure should be introduced explicitly in calculations of the non-Newtonian flow field with the help of the Stokes equation and PGD.

Practically, thermoplastic polymers showing the shear-thinning behavior maintain a finite constant viscosity at small strain rate up to a certain value. Therefore, the dependence of the viscosity on the shear rate will be modeled with the help of the Carreau-Yasuda viscosity model, which was extended from the Carreau model by Yasuda in 1979, who added one more parameter a to improve the degree of fit:

$$\mu = \mu_\infty + \frac{\mu_0 - \mu_\infty}{\left[1 + (\dot{\gamma} t_c)^a\right]^{\frac{1-n}{a}}}, \tag{7}$$

where μ_0 is the zero-shear viscosity, μ_∞ is the infinite-shear viscosity. The adjustment of the parameter a, when $a > 1$, allows to prescribe the length of the low-shear viscosity plateau, i.e. the maximal shear rate until which the fluid demonstrates the Newtonian behavior. t_c is also a parameter that controls the onset of the non-Newtonian behavior, namely by participating in the expression $\dot{\gamma} = 1/(t_c\sqrt{2-n})$ defining the point of inflexion of the viscosity-shear rate curve.

According to the procedure of non-linear iterations, the viscosity field is recalculated depending on the strain rate $\dot{\gamma} = \sqrt{2(\mathbf{D} : \mathbf{D})}$, where $\mathbf{D}$ is the strain rate tensor. It should be noted that in order to introduce the viscosity field into the PGD computation of the Stokes flow, the viscosity field should be represented in the separated form, which was done by the Singular Value Decomposition (SVD) procedure with the precision of 10^{-7}.

The resolution of the transverse generalized fluid flow through the aligned fiber bundles showed the 2D character of the velocity field – see streamlines in the plane perpendicular to the fibers axes in (Fig. 4a), as well as of the viscosity field – see the viscosity distribution in the transverse cross-sections in (Fig. 4b). This allows to reduce the problem to the two-dimensional statement, and to perform the calculations with the computational cost of one-dimensional problems because it includes only 1D functions in the separated representation.

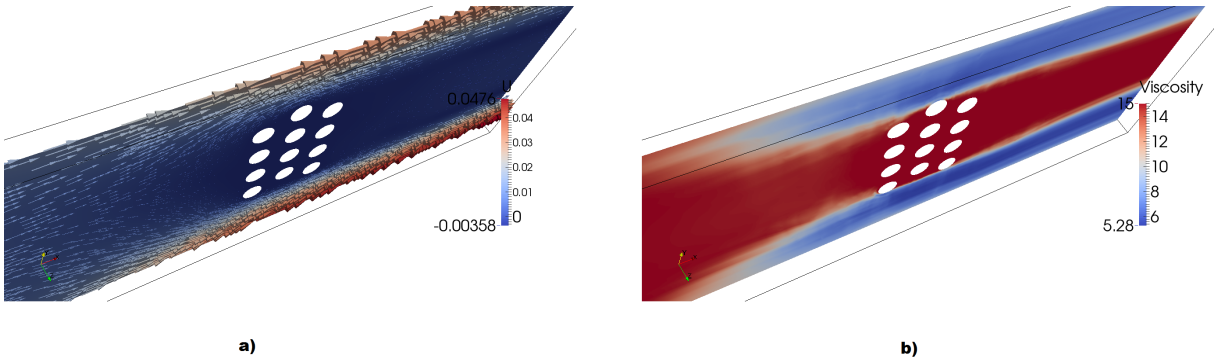

Figure 4. a) Streamlines with 2D character; b) viscosity field in the parallel to the flow cut.

A number of parameters were checked for their influence on the resultant viscosity field inside and outside the fiber bundles, one of the main objectives being to investigate the presence/absence of eventual shear-thinning effects inside the yarns. Imposing the periodicity boundary conditions on the representative domain with two fiber bundles (Fig. 5: the resin flows from the left-hand side perpendicularly to the fiber bundles axes), and varying the distance between the bundles in the parallel and perpendicular direction to the direction of flow showed that this meso-parameter does not affect the viscosity values inside the micro-structure.

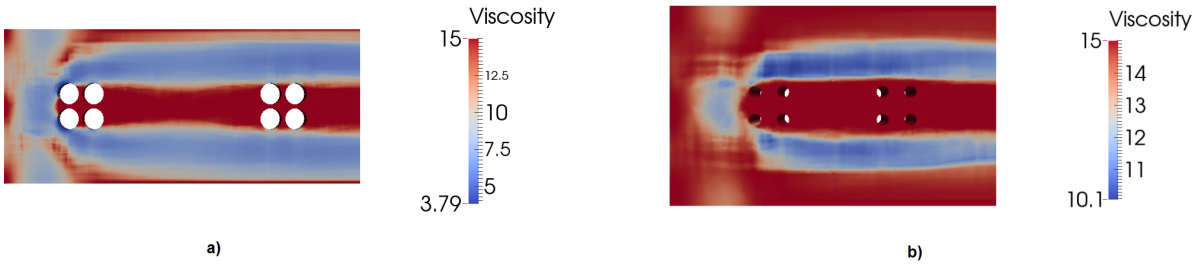

Figure 5. Viscosity fields (Carreau-Yasuda parameters $n = 0.4$, $\mu_0 = 15Pa \cdot s$, $\mu_\infty = 0.001Pa \cdot s$, $t_c = 0.007s$, $a = 5$) for different levels of fiber compaction within the yarns: a) 0.25Δ; b) 2Δ, where $\Delta = 14.6\mu m$.

The viscosity field inside the fiber bundles is influenced by another geometrical parameter – the distance Δ between the fibers inside the yarn, which was set to the value of $14.6\mu m$ and varied in the range 0.25Δ, Δ, and 2Δ. The Carreau-Yasuda model parameters: $n = 0.4$, $\mu_0 = 15Pa \cdot s$, $\mu_\infty = 0.001Pa{\cdot}s$, $t_c = 0.007s$, $a = 5$ were kept constant. The prescribed viscosity law implies the onset of shear-thinning effects after the shear rate reaches 100 s^{-1}. The range of the viscosity values in the resultant field was found to increase with the decreasing Δ (Fig. 5, Table 1). It means more significant deviation of the viscosity values from the initial Newtonian value μ_0 with the decrease of Δ. It is explained by the fact that closer packing of fibers induces more shear effects in the flow, and thus lower viscosity values. Since the resultant viscosity values range varies with the change of the level of packing of fibers within the yarn, it is more natural to estimate the Newtonian/non-Newtonian flow behavior inside the yarns taking as a reference the viscosity range $[\mu_{mindomain}; \mu_0]$ appropriate to each resolved domain according to: $(\mu_0 - \mu_{minfib})/(\mu_0 - \mu_{mindomain}) \cdot 100\%$, where μ_{minfib} is the minimal predicted value of the viscosity between fibers, $\mu_{mindomain}$ is the minimal predicted value of the viscosity in the whole domain. The results of estimation are presented in Table 1. With the increase of the level of fiber packing

Distance between fibers ($\Delta = 14.6\mu m$)	Deviation from the Newtonian viscosity value μ_0, % $(\mu_0 - \mu_{min\,fib})/(\mu_0 - \mu_{min domain}) \cdot 100\%$	Viscosity range, $Pa \cdot s$
0.25Δ	11.60%	3.79 - 15 (Fig. 5a)
Δ	8.26%	5.32 - 15
2Δ	0.02%	10.07 - 15 (Fig. 5b)

Table 1. Estimation of the non-Newtonian character of flow inside the fiber bundles with respect to the distance between the fibers.

within the yarns the viscosity inside the yarns deviates more from the initial Newtonian value. However, the deviation tendency is very slow compared to the increase of packing degree. Depending on the application cases, one or another percentage of deviation may be considered as a criterion to neglect the non-Newtonian effects in the flow within the fiber bundles.

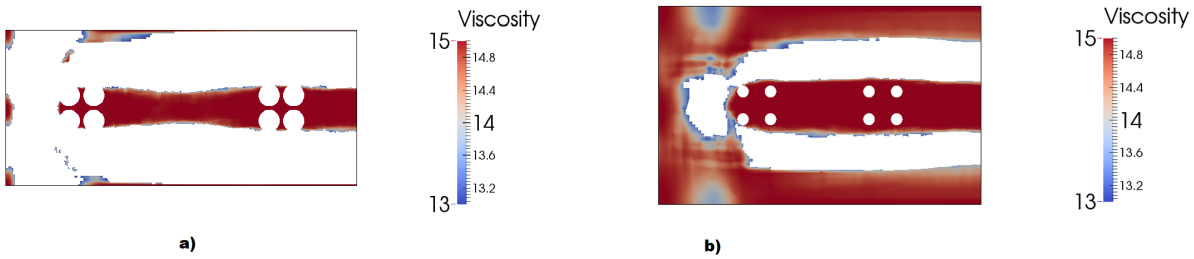

Figure 6. Distribution of the viscosity values in the range $13 - 15 Pa \cdot s$ – with the maximal deviation of 13% from the prescribed Newtonian viscosity value 15 $Pa \cdot s$ - for different levels of fiber compaction: a) 0.25Δ; b) 2Δ, where $\Delta = 14.6\mu m$.

The variation of different geometrical parameters showed that the higher difference between the characteristic channel size at micro-scale (between fibers) and characteristic channel size at meso-scale (between yarns), the more significant shear rates appear in the meso-domain.

The analysis of the performed calculations of the non-Newtonian resin flow perpendicularly to the aligned fiber bundles revealed the situations when the viscosity field between the fibers within the yarns stays constant conserving the initially prescribed viscosity value. In that case it means that now the Brinkman equation, taking into account the multi-scale nature of textile reinforcements, can be employed for modeling the non-Newtonian resin flow as follows:

$$\nabla p = \mu(\dot{\gamma})\nabla^2 \mathbf{u} - \phi\mu_0 K^{-1} \cdot \mathbf{u}, \tag{8}$$

where $\mathbf{u}$ is the intrinsic average fluid velocity; the Carreau-Yasuda law is prescribed for the viscosity change $\mu(\dot{\gamma})$ in the Stokes term, while in the second term, responsible for the fibrous domain, the constant viscosity μ_0 is fixed. This avoids the necessity to introduce explicitly in the calculations the fibrous microstructure – the information about it will be contained in the values of permeability K and porosity ϕ. For the fiber bundles with high fiber volume fraction the permeability can be calculated with the help of the relations derived in [4], specifying the radius of fibers, the fiber volume fraction, and the type of fiber packing (quadratic/hexagonal).

5. Conclusions

The Brinkman equation was selected for modeling the resin flow through the double-scale porosity textile reinforcements because it is capable of addressing several typical pore sizes: both the domain with larger pores – fluid channels between yarns, and the homogeneous domain of smaller pores – micro-channels between fibers. The methodology of resolution was based on the Proper Generalized Decomposition, which allowed to obtain high-accuracy solution with the reasonable computational time. Besides, thanks to the concept of separated representations in PGD, the data for the parametric study of influence of the ratio (also referred to as Darcy number) between the permeability of fibrous micro-domain and the square of the characteristic void size of meso-domain were obtained in one-shot calculation for the whole range of parameters. It was found that when this ratio approximately equals to 10^{-3} the character of the flow changes: smaller than 10^{-3} values imply that the flow through the micro-channels between the fibers can be neglected comparably to the flow through the meso-channels between the yarns.

Next step was to complexify the problem with the non-Newtonian behavior of flow through the double-scale porosity textile reinforcements. Since two terms of the Brinkman equation, describing two domains at different scales, require different viscosities to be specified, the Stokes equation was used to calculate the viscosity field of non-Newtonian fluid flowing through the fiber bundles. Under the conditions of not highly packed fibers within the yarns (inter-fiber distance $\geq$ fiber diameter) the flow between fibers was shown to have a Newtonian character. It can be concluded that the Brinkman equation can be applied under these conditions for the calculation of the non-Newtonian resin flow through the fibrous preform, by specifying the viscosity change dependent on the shear rate law in the Stokes term, and the constant viscosity, equal to the initial value, in the second term. Hence the fibrous microscopic architecture does not need to be explicitly input in the model anymore.

Acknowledgments

The European Commission is gratefully acknowledged for the financial support received through the large-scale integrating collaborative project MAPICC 3D (Nr. 263159).

References

[1] F. Chinesta, A. Ammar, A. Leygue, and R. Keunings. An overview of the proper generalized decomposition with applications in computational rheology. *Journal of Non-Newtonian Fluid Mechanics*, 166(11):578–592, 2011.

[2] C. L. Tucker III and R. B. Dessenberger. *Flow and Rheology in Polymer Composites Manufacturing*, chapter Governing equations for flow and heat transfer in stationary fiber beds. Elsevier Science Publishers, 1994.

[3] A. Leygue and E. Verron. A first step towards the use of proper general decomposition method for structural optimization. *Archives of Computational Methods in Engineering*, 17(4):465–472, 2010.

[4] B.R. Gebart. Permeability of unidirectional reinforcements for rtm. *Journal of Composite Materials*, 26(8):1100–1133, 1992.